Available online at www.sciencedirect.com
ScienceDirect
Journal of Nuclear Materials 373 (2008) 335–342
journal of nuclear materials
www.elsevier.com/locate/jnucmat

Some physical data of the near eutectic liquid lead–bismuth

Yu. Plevachuk [a], V. Sklyarchuk [a], S. Eckert [b], G. Gerbeth [b,*]

[a] Ivan Franko National University, Faculty of Physics, 8 Kyrylo and Mephodiy Street, 79005 Lviv, Ukraine
[b] Forschungszentrum Dresden-Rossendorf, Institute of Safety Research, P.O. Box 510119, D-01314 Dresden, Germany

Received 13 February 2007; accepted 14 June 2007

Abstract

Lead–bismuth alloys are under intense consideration as target material of spallation sources. The thermohydraulic design of such a target or related coolant systems requires a reliable data basis regarding the temperature dependent physical properties of such alloys. We present measurements of the electrical conductivity and thermoelectric power up to about one hundred degree above the melting point for various alloy compositions. For the eutectic alloy, the measurements were performed up to much higher temperatures including, in addition, viscosity, thermal conductivity and surface tension. A comparison with data and scaling relations available in literature is given.

PACS: 65.20.+w; 66.20.+d; 72.15.Cz

1. Introduction

Lead–bismuth alloys are of recent interest for spallation neutron targets [1–3]. Various target designs are under consideration including the set-up and instrumentation of related liquid metal loops [2,4,5]. Obviously, for the design of such targets a reliable knowledge of relevant alloy properties is mandatory. Investigations on different alloy characterizations are, therefore, a continuous and recent subject of research [6–9].

The physical properties, such as density, viscosity, thermal and electrical conductivity or specific heat, are of direct relevance for the thermohydraulic design of a Pb–Bi target and the related liquid metal loop. Several reviews of those data exist. Former measurements performed in Russia have been summarized in the book of Kutateladze et al. [10]. Cevolani and Tinti [11] performed in 1998 a literature review resulting in suggested temperature scalings, which are often used meanwhile. The recent paper of Morita et al. [12] presented data mainly on density, the vapor pressure curve and the vapor equation of state, but included also some literature data on thermal conductivity, viscosity and surface tension. Due to the recent interest in Pb–Bi targets, further literature reviews of the interesting material data exist, see for instance the report [13] or very recently the review of Sobolev [14]. However, the discrepancy between the reported results, different investigated temperature ranges, and sometimes a very limited number of measuring points require new precise measurements in order to obtain reliable data on the temperature dependence of the above mentioned thermophysical properties over a wide temperature range.

In the present paper, new measurements are reported on the electrical conductivity, the thermopower, the viscosity, the thermal conductivity, and the surface tension of the eutectic Pb–Bi alloy in the temperature range between 400 and 1000 K. Related temperature correlation fits are derived and compared with those available in literature. In addition, the electrical conductivity and the thermoelectric power are given for Pb–Bi alloys of varying compositions. Of particular interest, thereby is the melting–solidification range of temperatures, where some hysteresis is observed depending on the heating–cooling cycles.

* Corresponding author. Tel.: +49 351 2603484; fax: +49 351 2602007.
E-mail address: g.gerbeth@fzd.de (G. Gerbeth).

0022-3115/$ - see front matter © 2007 Elsevier B.V. All rights reserved.
doi:10.1016/j.jnucmat.2007.06.014

2. Measuring methods

2.1. Electrical conductivity and thermoelectric power

The electrical conductivity, $\sigma(T)$, and the thermoelectric power, $S(T)$, were measured by a contact method with a 4-point scheme. According to this scheme the potential drop U is measured at two electrodes located along a straight line between the electrodes carrying the electric current I. Then, the electrical conductivity is determined by $\sigma = Il/US$, where l is the length and S is the cross-section of the sample. When it was difficult to determine precisely the geometric dimensions, σ was found from $\sigma = IG/U$, where G is the geometrical factor, which has been conveniently determined by calibration with mercury.

The experiments were performed in an argon atmosphere. Graphite electrodes for current and potential measurements were placed in the wall of the vertical cylindrical BN-ceramic measuring cell along its vertical axis. The potential electrodes were provided with thermocouples for temperature measurements. Single thermoelectrodes of these thermocouples were used for electrical conductivity and thermoelectric power determination. The melt temperature was determined by WRe-5/20 thermocouples in close contact with the liquid. Temperature gradients of 3–4 K/cm along the cell were additionally controlled to be within 0.1 K by a preliminary calibrated 5-point differential thermocouple. The cell construction permits to carry out the electrical conductivity and thermoelectric power measurements simultaneously in one run. For further details of this method and its experimental realization we refer to Ref. [15].

Pure Pb and Bi were melted and evacuated in sealed quartz ampoules at 10–15 Pa. Then each sample was inserted into the cell directly inside a high-pressure vessel. Thus, the sample composition was accurate within 0.02 wt%. The resultant error of the electrical conductivity measurements is about 2%, and about 5% for the thermoelectric power determination.

2.2. Viscosity

The measurements of the viscosity were carried out using a computer-controlled oscillating-cup viscosimeter [16]. Using the Roscoe equation [17], the dynamic viscosity, $\eta(T)$, has been calculated from the corresponding logarithmic decrement and the period of oscillations. The experiments were performed in helium atmosphere under a negligible excess pressure of about 0.02–0.03 MPa. The sample compositions of about 30 g were accurate to 0.02 wt%. Each sample has been weighed before and after the measurements, and no loss of mass has been observed. Cylindrical graphite crucibles with internal diameter of 14 mm were used. A homogeneous temperature field up to 0.3 K in the range of absolute values up to 800 K has been created inside the furnace. The temperature has been measured with a WRe-5/20 thermocouple arranged just below the crucible. The viscosity was measured with an accuracy of about 3%.

2.3. Thermal conductivity

An experimental arrangement based on the steady-state concentric cylinder method was used for thermal conductivity measurements [18]. The apparatus comprises two coaxial cylinders (stainless steel, BN or graphite) separated by a gap, into which the melt is poured. A central hole is drilled in the inner cylinder for an internal heater made of a molybdenum wire, wound on an alumina form. The inner heater is used for producing the necessary temperature gradient in the investigated melt layer. The cell is closed by a BN cover, which is sealed with a special compound based on a finely dispersed BN powder. The outer three-section furnace is made of molybdenum wire wound on a BN form. The outer heater produces an over-all temperature level, and its upper and lower sections permit regulation of the temperature field over the height of the apparatus. Tungsten–rhenium WR5/20 thermocouples were used in the experiments. Two thermocouples placed in the body of the inner cylinder allow the examination of the temperature distribution over the radius of the apparatus. The coefficient of thermal conductivity, $\lambda(T)$, can be calculated from the formula for the heat transfer in a cylindrical layer. The design of the apparatus assures a maximum reduction of the heat leakage and of convection. The resultant error of thermal conductivity measurements is about 7%.

2.4. Surface tension

The surface tension was measured using a 'large drop' method in the temperature range between T_m and 1000 K. The method is a modification of the sessile drop method and allows overcoming problems connected with a large sessile drop asymmetry [19]. This modification of the sessile drop technique has two advantages, namely it produces a large axisymmetric meniscus and can be used with both wetting and non-wetting systems. Besides, a drop enlargement allows to reduce the experimental uncertainty by almost one order of magnitude. A circular crucible, which has its upper circumferential edge chamfered to an acute angle, is overfilled with fluid, so that an axisymmetric meniscus, with a diameter exceeding the diameter of the crucible is produced and stands proud of the rim. The experiments were performed in an atmosphere of 90%Ar + 10%H_2 after initially evacuating the working volume of the chamber in order to avoid sample oxidation.

The temperature has been measured with the WRe5/20 thermocouple placed near the specimen and was kept constant within 1 K. A CCD camera and a computer-controlled equipment were used for determination of the drop parameters. Based on the Laplace–Young equation, the surface tension, $\gamma(T)$, was calculated by the Kozakevitch

method [20]. The surface tension data were obtained with an accuracy of about 0.5%.

3. Results and discussion

3.1. Electrical conductivity and thermoelectric power

For these measurements, the alloys $Pb_{40}Bi_{60}$, $Pb_{50}Bi_{50}$, and the eutectic composition $Pb_{44}Bi_{56}$ (at.%) have been chosen for investigation. Additional studies were carried out for the alloys $Pb_{43}Bi_{57}$, $Pb_{45}Bi_{55}$, and $Pb_{46}Bi_{54}$, the compositions of which are very close to the eutectic one. One motivation for it consisted in a slight discrepancy in the reported eutectic compositions, ranging from $Pb_{42.6}$-$Bi_{57.4}$ to $Pb_{45}Bi_{55}$ [7,21–23]. In the following, any reference to a phase diagram of the considered Pb–Bi alloys always relates to the phase diagrams given in Ref. [21].

The electrical conductivity $\sigma(T)$ and the thermoelectric power $S(T)$ of the liquid $Pb_{40}Bi_{60}$ alloy are presented in Fig. 1. A solidification range from 444 K to 411 K has been revealed. The melting and solidification processes are accompanied by a hysteresis. Fig. 1 presents the results of a third melting–solidification cycle. It was found that thermocycling increased the temperatures of the melting completion as well as of the solidification start, compared to the liquidus temperature $T_L = 417$ K indicated by the phase diagram. As confirmed by both the electrical conductivity and thermoelectric power data, the overheating can reach almost 40 K. A first small jump on the $\sigma(T)$ and $S(T)$ curves has been observed during melting of the $Pb_{40}Bi_{60}$ at 402 K. A kink at about 432 K is probably connected with reaching the maximum concentration of the crystalline phase. This is reflected at the $S(T)$ behaviour as a sign change of the temperature coefficient of the thermoelectric power (dS/dT). It is suggested that the melting ends at about 464 K. Beginning from this temperature, the electrical conductivity is weakly temperature dependent and decreases with further heating. After melting, the thermoelectric power is practically temperature independent. The cooling $S(T)$ curve almost coincides with the heating one, but the solidification starts at approximately 444 K. It should be noted that the solidification temperature determined from the $S(T)$ data is 396 K, i.e. 2.5 K below the eutectic melting temperature $T_m = 398.5$ K.

Thermocycling of the $Pb_{50}Bi_{50}$ liquid alloy had no influence on the liquidus and solidus temperatures (Fig. 2). The liquidus (423 K) and the solidus (400 K) temperatures were the same both for melting and solidification. A jump in the $d\sigma/dT$ curve was observed at 413 K. Generally, the $\sigma(T)$ behaviour is similar to that for pure Pb. No peculiarities were also observed at the $S(T)$ dependence except for the undercooling of about 5.5 K below the solidus.

The properties of the eutectic composition $Pb_{44}Bi_{56}$ are also similar to those of pure lead (Fig. 3). The electrical conductivity decreases with increasing temperature, falls drastically at the melting temperature, T_m, then decreases linearly with further temperature increase. Nevertheless, an influence of thermocycling is noticeable, and each following heating shifts the T_m to higher values (up to 5 K). Solidification starts at the eutectic temperature and its range does not exceed 4–5 K. The influence of thermocycling was also observed in the $S(T)$ curve.

The investigated temperature range for the eutectic composition was not limited to the melting–solidification range but extended to higher temperatures up to 1000 K. As seen from Fig. 4 the electrical conductivity decreases linearly upon heating in the temperature range between T_m and approximately 600 K according to:

$$\sigma = \sigma_0 + \frac{d\sigma}{dT} \times (T - T_m), \quad (1)$$

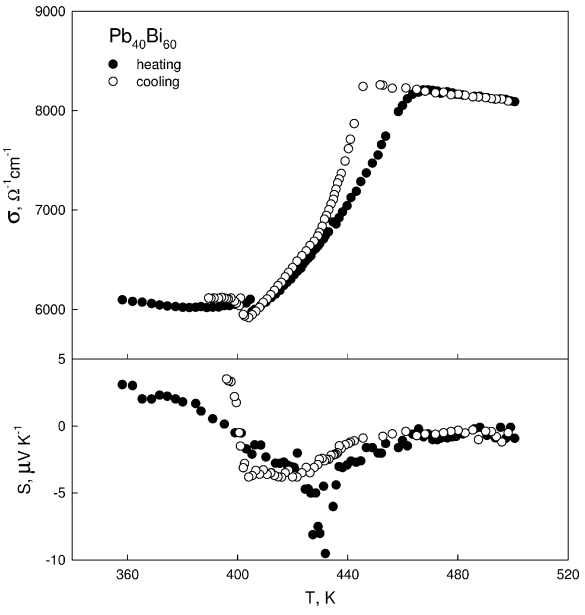

Fig. 1. Electrical conductivity and thermoelectric power vs. temperature for the $Pb_{40}Bi_{60}$ liquid alloy.

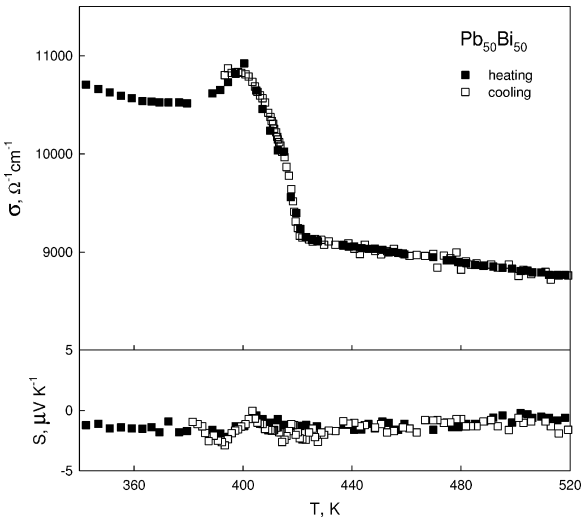

Fig. 2. Electrical conductivity and thermoelectric power vs. temperature for the $Pb_{50}Bi_{50}$ liquid alloy.

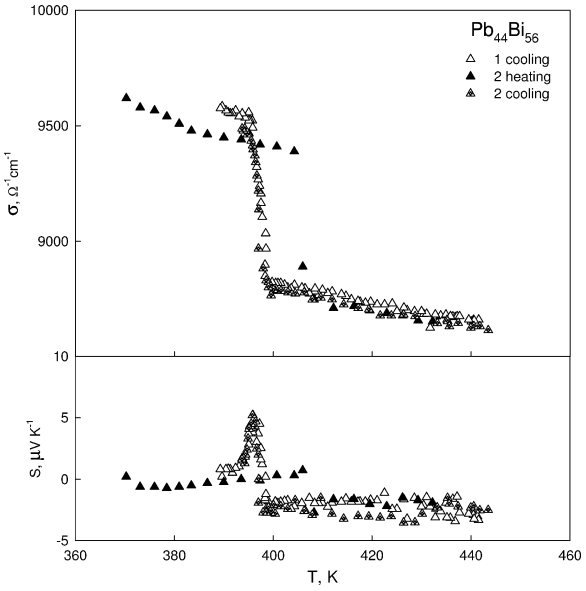

Fig. 3. Electrical conductivity and thermoelectric power vs. temperature for the eutectic $Pb_{44}Bi_{56}$ liquid alloy.

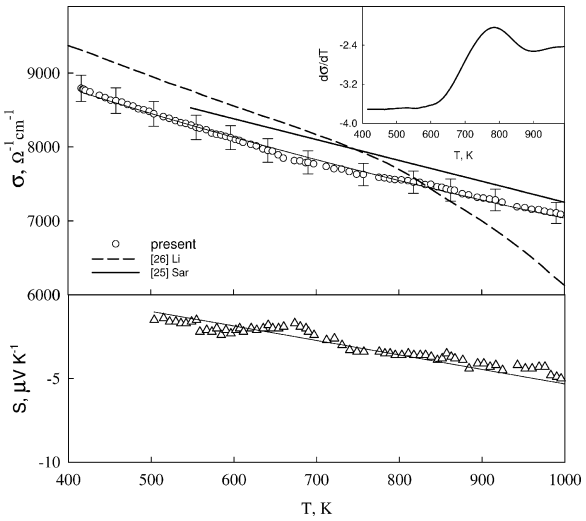

Fig. 4. Electrical conductivity and thermoelectric power vs. temperature for the eutectic $Pb_{44}Bi_{56}$ liquid alloy in an extended temperature range and compared to literature data.

where $\sigma_0 = 8847.57\ \Omega^{-1}\ \mathrm{cm}^{-1}$ is the electrical conductivity at the melting point and $\mathrm{d}\sigma/\mathrm{d}T = -3.69\ \Omega^{-1}\ \mathrm{cm}^{-1}\ \mathrm{K}^{-1}$ is the temperature coefficient of conductivity. The linearity in this temperature range was also reported in [24–26]. It is seen in Fig. 4, that a difference between our values and the higher values from [26] (converted from resistivity to conductivity) is typically in the range of 5% with a very similar negative slope. The data from [25] are also slightly higher, but in better agreement with ours.

Extending the temperature range, we observed some anomalies in the $\sigma(T)$ curve, which are more evident in the $\mathrm{d}\sigma/\mathrm{d}T = f(T)$ dependence as shown in the inset of Fig. 4. Similar peculiarities for the Pb–Bi liquid alloys were also observed recently [26], but the general run of the $\sigma(T)$ curve differs. Such a deviation from linearity at temperatures considerably higher than T_m suggests a structure inhomogeneity of the melt and requires closer examination, which is, however, beyond the scope of the present paper.

The temperature dependence of the electrical conductivity (in units of $\Omega^{-1}\,\mathrm{cm}^{-1}$) in the extended temperature range between T_m and 1000 K can be interpolated by the quadratic relationship:

$$\sigma = 8803.41 - 3.5228(T - T_m) + 9.8112 \times 10^{-4}(T - T_m)^2. \quad (2)$$

To a good approximation, the thermoelectric power decreases linearly with heating according to

$$S = S_0 - 8.6671 \times 10^{-3}(T - T_m), \quad (3)$$

where $S_0 = -0.1076\ \mu\mathrm{V/K}$ is the thermoelectric power at the melting point.

The results for the near eutectic compositions of $Pb_{43}Bi_{57}$ (Fig. 5), $Pb_{45}Bi_{55}$ (Fig. 6), and $Pb_{46}Bi_{54}$ (Fig. 7) are, actually, close to the eutectic case. A small temperature 'melting–solidification' hysteresis has been revealed in the $Pb_{46}Bi_{54}$ melt. Solidification of this melt began at approximately 402 K and came to the end at 390 K. The properties of the liquid alloys $Pb_{43}Bi_{57}$ and $Pb_{45}Bi_{55}$ are very similar to those of the eutectic one. The similar temperature dependencies of the electrical conductivity and the thermoelectric power suggest that the solidification processes in both the eutectic and the near eutectic (within 1–2 at.%) liquid alloys are almost identical.

Numerous studies are dedicated to melting and solidification processes in metal systems [27,28]. It was shown that only a very slow cooling ensures the equilibrium of the solidification process. The restriction of the thermodynamic equilibrium in course of melting–solidification is mainly determined by a finite velocity of the component diffusion in the liquid and solid phases. In reality, a restricted diffusion mass transfer leads to a non-equilibrium solidification, and the resulting solid solution is non-uniform in composition. Note that melting and solidification can be

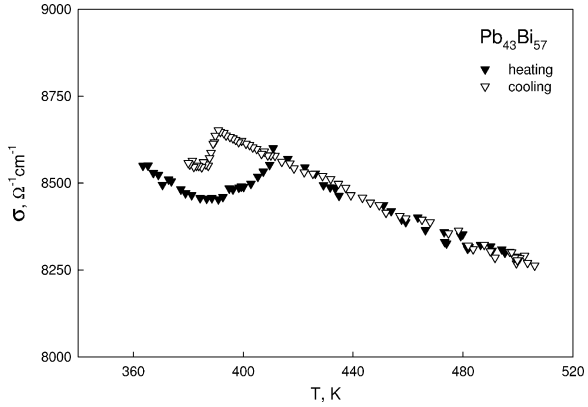

Fig. 5. Electrical conductivity vs. temperature for the $Pb_{43}Bi_{57}$ liquid alloy.

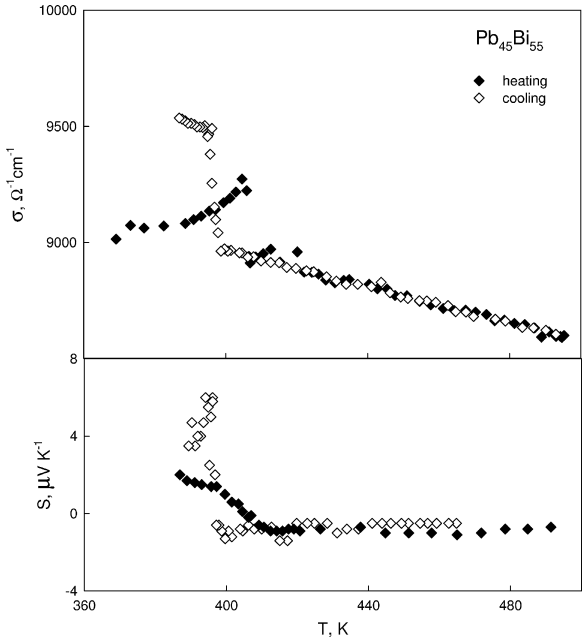

Fig. 6. Electrical conductivity and thermoelectric power vs. temperature for the $Pb_{45}Bi_{55}$ liquid alloy.

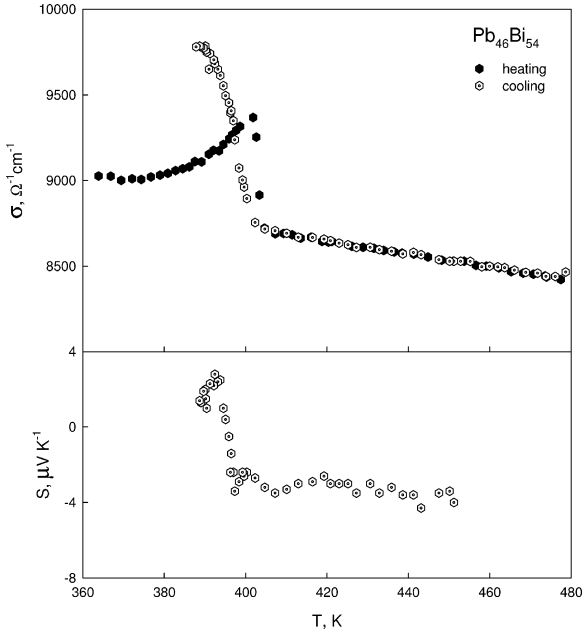

Fig. 7. Electrical conductivity and thermoelectric power vs. temperature for the $Pb_{46}Bi_{54}$ liquid alloy.

considered as reversible processes only when they occur in equilibrium.

Describing the alloys phase transformations one constructs often the lines of metastability running below the liquidus [22]. These lines correspond to the equilibrium between a liquid and a nucleus in some concentration region and are located on the extension of the liquidus line below the eutectic point. There are different ways of eutectic transformations depending on the initial alloy composition. As shown in Ref. [22], the following processes are possible:

(1) The first precipitated particles of the solid phase become the crystallization nuclei for another phase. In this case the eutectic transformation occurs at the eutectic temperature.
(2) These first precipitated particles do not become the crystallization nuclei for another phase, and the melt is not sensible to them. The particles continue to precipitate with decreasing temperature below the eutectic temperature, and the liquid composition changes along the extension of the liquidus line. In this case, the eutectic transformation occurs below the eutectic temperature.

Generally, the eutectic transformation occur either at the eutectic temperature or below it, depending on the influence of the first precipitates on the second liquid phase. An increase of the solidification velocity leads to an enlargement of the undercooling region.

3.2. Viscosity

The dynamic viscosity of the eutectic composition $Pb_{44}Bi_{56}$ was measured during heating and cooling over a wide temperature range between 400 and 1000 K in steps of 5 K. Several experiments with different samples of the same composition revealed a good reproducibility of the results. The dynamic viscosity as a function of temperature is presented in Fig. 8 together with data of other authors.

Fitting the measured viscosity values (in units of mPa·s) to an Arrhenius equation

$$\eta(T) = \eta_0 \exp\left(\frac{E}{RT}\right), \tag{4}$$

where T is taken in K and $R = 8.3144$ J/K mol is the gas constant, results in the following fit parameters: $\eta_0 = 0.5886$ and $E = 5.845$ kJ/mol. This fit is shown in Fig. 8 as a full line.

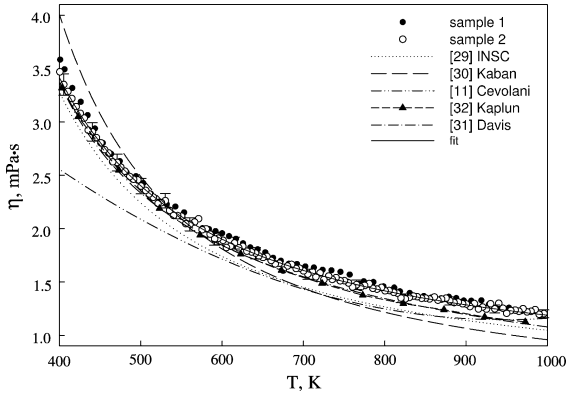

Fig. 8. Dynamic viscosity vs. temperature for the eutectic $Pb_{44}Bi_{56}$ liquid alloy, compared to literature data.

We compare our results with viscosity data collected in two recent reviews [11,29] as well as from other papers [30,31]. It turns out that the fit of Cevolani and Tinti [11]

$$\eta = 3.26 - 6.26 \times 10^{-3} T + 4.63 \times 10^{-6} T \quad (5)$$

always underestimates the viscosity values. The difference is typically in the range of 10% (about 13% at 500 K and about 9% at 800 K), but reaches about 25% at the lower temperature of $T = 400$ K. It is worth to note that the present results are in a much better agreement with the data from Kutateladze et al. [10], which were also cited in [11], but not further taken into account there.

The data from the International Nuclear Safety Center [29] look more trustworthy because of the described uncertainties and the careful evaluation of the data. Although the cited data from different sources were in good agreement, only the data from Kaplun et al. [32], fitted by the Arrhenius equation $\eta = 0.4656 \exp(773.2/T)$ were selected [29] for the final recommended fitting equation, which is also of the Arrhenius type: $\eta = 0.49 \exp(760.1/T)$.

The viscosity values based on the ATHENA code calculations [31] are slightly higher compared to the values from the equation proposed in [29], but coincide with the data of Kutateladze et al. [10]. The $\eta(T)$ curve obtained in [30] is more abrupt, but the data agree with those from [29–31,10] between 450 and 1000 K within the limits of the reported experimental errors and are well described by the Arrhenius equation $\eta = 0.37 \exp(7.92/RT)$.

As mentioned in Section 2, the viscosity measurement uncertainty of our data is about 3%. The additional uncertainty caused by fitting the data into Eq. (4) is about 2.7%. The total uncertainty might be estimated as the square root the sum of the squares of the separate uncertainties, resulting in about 4% uncertainty for the finally obtained data fit. Taking into account the upper and lower limits of all the reported uncertainties, the present data are in agreement with the data of [10,29–32]. The different slope of the $\eta(T)$ curve in [30] in the lower temperature range might be explained by experimental peculiarities of the measuring method applied in [30]. Thus, most of the reported viscosity results are well described by an Arrhenius equation. Only the relationship proposed in [11] differs.

3.3. Thermal conductivity

The temperature dependence of the thermal conductivity $\lambda(T)$ was measured in the temperature range from the melting point up to 1000 K. As seen from Fig. 9, just above the melting point the present data and the slope are in agreement with the data reported in Ref. [33]. Beginning from about 500 K, a deviation from linearity appears, and the slope of the $\lambda(T)$ curve changes. At higher temperatures the data are very close to those reported in [34,35].

The measurements of Kutateladze et al. [10] indicate lower values for the thermal conductivity below approximately 500 K and higher values above this temperature. The data of [34,36] are higher and the data of [35] are

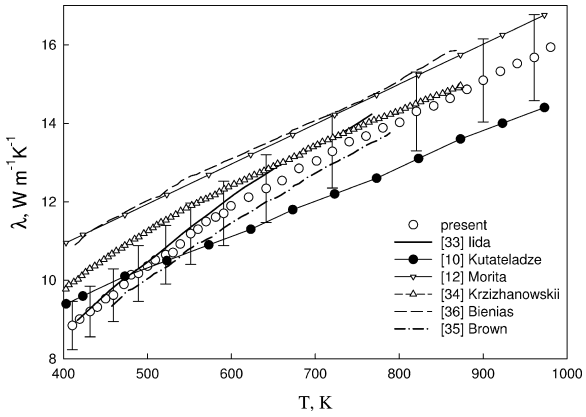

Fig. 9. Thermal conductivity vs. temperature for the eutectic $Pb_{44}Bi_{56}$ liquid alloy, compared to literature data.

lower. However, the discrepancy falls within the combined experimental uncertainties of the various measurements (present – 7% error, [34] – 10% error). Finally, the present study did not confirm a piecewise linear form of the $\lambda(T)$ curve as suggested by the ATHENA calculations [31].

The thermal conductivity values resulting from our measurements might be summarized by the following fit:

$$\lambda = 0.7158 + 0.0233\ T - 8.1098 \times 10^{-6} T^2, \quad (6)$$

where λ is in units of $W\,m^{-1}\,K^{-1}$ and the temperature is in K.

3.4. Surface tension

Surface tension measurements of the molten eutectic $Pb_{44}Bi_{56}$ were performed between the melting point T_m and 1000 K. The surface tension data vs. temperature $\gamma(T)$ are shown in Fig. 10 together with data for pure Pb, Bi and results of previous studies [12,37–42]. Although

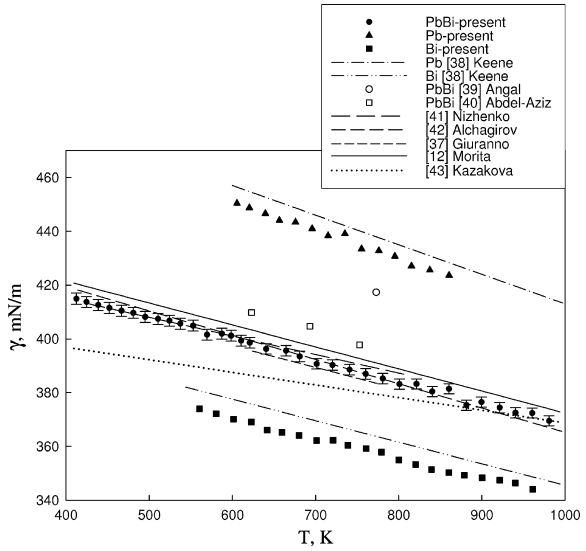

Fig. 10. Surface tension vs. temperature for the eutectic $Pb_{44}Bi_{56}$ liquid alloy and for pure Pb and Bi, compared to literature data.

many authors reported surface tension reference data for Pb and Bi, the data are often rather contradictory because of experimental difficulties, the peculiarities of each measurement method employed and a wide scatter in experimental errors (0.1–7%). Even more, the surface tension of the Pb–Bi melts appears as imperfectly studied (see [37] and references therein).

Usually the surface tension decreases linearly with increasing temperature, and can be presented as $\gamma = \gamma_0 - (\frac{d\gamma}{dT}) \times (T - T_m)$, where γ_0 is the surface tension at the melting temperature T_m and $d\gamma/dT$ is the temperature coefficient of the surface tension. The data obtained by our measurements can be interpolated by the relationship:

$$\gamma = 416.208 - 0.0799 \times (T - T_m), \quad (7)$$

where γ is in units of mN/m. This relation is very close to the expression $\gamma = 413.519 - 0.0801 \times (T - 398)$ reported in Ref. [37].

As seen from Fig. 10, the present surface tension values are also close to the data reported in [41,42]. Slight differences exist to the results of [40,43], but the deviations never exceed 5%. It is worth to note that almost all results, except [43], give in a good approximation the same value for the surface tension temperature coefficient. The calculated $\gamma(T)$ curve [12] as

$$\gamma = 453.7 \times \left(1 - \frac{T}{T_c}\right)^{0.8640}, \quad (8)$$

where $T_c = 4890$ K is the critical temperature, is located slightly above the experimental data. In general, the experimental studies fit always to a linear temperature dependence of the surface tension of the Pb–Bi eutectic melt. The present investigation carried out in an extended temperature range confirms this result.

4. Conclusion

Several physical properties of the liquid eutectic alloy PbBi have been measured in the temperature range from the melting point up to 1000 K. Corresponding fit relations have been derived for the electrical conductivity (Eq. (2)), the thermoelectric power (Eq. (3)), the dynamic viscosity (Eq. (4)), the thermal conductivity (Eq. (6)) and the surface tension (Eq. (7)). All properties are compared to available literature data. In addition, the electrical conductivity and the thermoelectric power up to about 100 K above the melting point have been determined also for several compositions around the eutectic one. The investigations revealed the anomalies of the electrical conductivity and thermoelectric power vs. temperature curves, such as hysteresis and heating–cooling curve divergence. The undercooling of the melts with compositions shifted opposite with respect to the eutectic one occurs at different temperatures. An influence of thermocycling is noticeable for some alloys, and each following cycle shifts the melting point to higher values.

Acknowledgements

The authors acknowledge Deutsche Forschungsgemeinschaft in frame of the Collaborative Research Centre SFB 609 for the financial support of this work. Support by the European Commission in frame of the EUROTRANS project under Contract FI6W-CT-2004-516529 is gratefully acknowledged.

References

[1] B.F. Gromov, Yu.S. Belomitcev, E.I. Yefimov, M.P. Leonchuk, P.N. Martinov, Yu.I. Orlov, D.V. Pankratov, Yu.G. Pashkin, G.I. Toshinsky, V.V. Chekunov, B.A. Shmatko, V.S. Stepanov, Nucl. Eng. Des. 173 (1997) 207.
[2] G.S. Bauer, M. Salvatores, G. Heusener, J. Nucl. Mater. 296 (2001) 17.
[3] R.G. Ballinger, J. Lim, Nucl. Technol. 147 (2004) 418.
[4] X. Cheng, I. Slessarev, Nucl. Eng. Des. 202 (2000) 297.
[5] C.B. Davis, Nucl. Eng. Des. 224 (2003) 149.
[6] Y. Gohar, J. Nucl. Mater. 318 (2003) 185.
[7] A.-M. Azad, J. Nucl. Mater. 341 (2005) 45.
[8] R.A. Khairulin, K.M. Lyapunov, A.G. Mozgovoi, S.V. Stankus, P.V. Ulyusov, J. Alloys Comp. 387 (2005) 183.
[9] R. Ganesan, T. Gnanasekaran, R.S. Srinivasa, J. Nucl. Mater. 349 (2006) 133.
[10] S.S. Kutateladze, V.M. Borishanskii, I.I. Novikov, O.S. Fedynskii, Liquid-metal heat transfer media, Atomizdat, Moscow, 1958.
[11] S. Cevolani, R. Tinti, ENEA technical report DT.SBD.00004 (1998).
[12] K. Morita, W. Maschek, M. Flad, Y. Tobita, H. Yamano, J. Nucl. Sci. Technol. 43 (5) (2006) 526.
[13] Comparative assessment of thermophysical and thermohydraulic characteristics of lead, lead–bismuth and sodium coolants for fast reactors, IEAEA report IAEA-TECDOC-1289, IAEA, Vienna, 2002.
[14] V. Sobolev, J. Nucl. Mater. 362 (2007) 235.
[15] Yu. Plevachuk, V. Sklyarchuk, Meas. Sci. Technol. 12 (1) (2001) 23.
[16] Yu. Plevachuk, V. Sklyarchuk, A. Yakymovych, B. Willers, S. Eckert, J. Alloys Comp. 394 (2005) 63.
[17] R. Roscoe, Proc. Phys. Soc. 72 (1958) 576.
[18] V. Sklyarchuk, Yu. Plevachuk, Meas. Sci. Technol. 16 (2005) 467.
[19] Yu.V. Najdich, Contact Phenomena in Metallurgical Melts, Naukova Dumka, Kyiv, 1972.
[20] P. Kozakevitch, in: J.O'M. Bockris, J.L. White, J.D. Mackenzie (Eds.), Physico Chemical Measurements at High Temperatures, Butterworth Science Publishers, London, 1959, Chapter 9, p. 208.
[21] T.B. Massalski (Ed.), Binary Alloy Phase Diagrams, ASM International, Materials Park, OH, 1996.
[22] S.S. Kutateladze, V.E. Nakoryakov (Eds.), Phase Transitions in Pure Metals and Binary Alloys, Academy of Sciences of the USSR Siberian Branch, Institute of Thermophysics, Novosibirsk, 1980.
[23] N.A. Gokcen, J. Phase Equilib. 13 (1992) 21.
[24] A. Roll, T.K. Biswas, Z. Metallkd. 55 (12) (1964) 794.
[25] F. Sar, These de doctorat, University Metz, 2005.
[26] Q. Li, F.Q. Zu, X.F. Li, Y. Xi, Mod. Phys. Lett. B 20 (4) (2006) 151.
[27] D.M. Herlach, Solidification and Crystallization, Wiley-VCH Verlag, Weinheim, 2004.
[28] W. Kurz, D.J. Fisher, Fundamentals of Solidification, third Ed., Trans Tech Publications, Switzerland, 1989.
[29] International Nuclear Safety Center, <http://www.insc.anl.gov/matprop/pbbi/pbbiviscosity.pdf>.
[30] I. Kaban, W. Hoyer, Yu. Plevachuk, V. Sklyarchuk, J. Phys.: Condens. Matter 16 (2004) 6335.
[31] C.B. Davis, A.S. Shieh, Overview of the use of ATHENA for analysis of lead–bismuth cooled reactors, in: Proceedings of the 8th International Conference on Nuclear Engineering (ICONE-8), 2–6 April 2000, Baltimore, MD.

[32] A.B. Kaplun, V.M. Shulaev, S.P. Linkov, Yu.D. Vartanov, The viscosity of the eutectic lead–bismuth alloyThe Thermophysical Properties of Substances and Materials, Kutateladze Institute of the Thermophysics of the USSR Academy of Sciences, Novosibirsk, 1979, p. 105.
[33] T. Iida, R.I.L. Guthrie, The Physical Properties of Liquid Metals, Oxford University, New York, 1993.
[34] R.E. Krzhizhanovskii, N.P. Sidorova, I.A. Bogdanova, J. Eng. Phys. Thermophys. 29 (2) (1975) 1046.
[35] W. Byron Brown, Phys. Rev. 22 (2) (1923) 171.
[36] A. Bienias, F. Sauerwald, Z. Anorg. Chem. 161 (1927) 51.
[37] D. Giuranno, F. Gnecco, E. Ricci, R. Novakovic, Intermetallics 11 (2003) 1313.
[38] B.J. Keene, Int. Mater. Rev. 38 (4) (1993) 157.
[39] R.D. Angal, Z. Metallkd. 73 (1982) 428.
[40] A.-H.K. Abdel-Aziz, M.B. Kirshah, Z. Metallkd. 68 (1977) 437.
[41] V.M. Nizhenko, L.I. Floka, Surface Tension of Liquid Metals and Alloys, Metallurgiya, Moscow, 1981.
[42] B.B. Alchagirov, A.M. Chochaeva, A.G. Mozgovoi, M.N. Arnoldov, V.B. Bekulov, Kh. B. Khokonov, High Temp. 41 (6) (2003) 755.
[43] I.V. Kazakova, S.A. Lyamkin, B.M. Lepinskikh, Russ. J. Phys. Chem. 58 (1984) 932.